International Journal of Mass Spectrometry 287 (2009) 39–45

Contents lists available at ScienceDirect

International Journal of Mass Spectrometry

journal homepage: www.elsevier.com/locate/ijms

A dual time-of-flight apparatus for an ion mobility-surface-induced dissociation-mass spectrometer for high-throughput peptide sequencing

Wenjian Sun, Jody C. May, Kent J. Gillig, David H. Russell*

Laboratory for Biological Mass Spectrometry, Department of Chemistry, Texas A&M University, College Station, TX 77843, United States

ARTICLE INFO

Article history:
Received 25 August 2008
Received in revised form 28 October 2008
Accepted 24 November 2008
Available online 3 December 2008

Keywords:
Ion mobility spectrometry
Mass spectrometry
Surface-induced dissociation
Time-of-flight
MS–MS

ABSTRACT

A novel ion mobility (IM)-surface-induced dissociation (SID)-mass spectrometer consisting of two independent time-of-flight (TOF) mass analyzers is described. The dual TOF instrument configuration facilitates high-throughput post-ionization separation and mass analysis of precursor and fragment ions, and the utility of 3D data acquisition is demonstrated for top-down proteomics by performing simultaneous acquisition of peptide mass maps and amino acid sequence determination.

1. Introduction

Analytical chemists have long recognized the potential for multi-dimensional data acquisition afforded by rapid advances in analysis and data processing capabilities of modern computers and computational techniques. Although computers are now regarded as integral components of modern analytical instruments, such concepts were once at the very forefront of analytical chemistry research. Many individuals contributed to the evolutionary development of the sub-discipline of analytical chemistry frequently referred to as computer-enhanced analytical chemistry, Charles Wilkins was a pivotal individual, both in terms of contributions to computerization of instrumentation and methodologies for data handling and spectral interpretation as well as dissemination of results and technological advances [1,2]. Today, the field of computer-enhanced analytical chemistry provides the foundations for the many rapidly developing methodologies and high-throughput techniques that drive the fields of genomics, proteomics, glycomics, metabolomics, lipidomics, petroleomics, and other emerging "omics" fields [3]. In addition, advances in computers and instrumentation facilitate development and application of multi-dimensional techniques such as chromatography–mass spectrometry, Fourier-transform mass spectrometry, ion mobility-mass spectrometry (IM-MS), tandem mass spectrometry, and combinations of these techniques with emerging areas such as molecular imaging mass spectrometry. Without the seminal contributions made by workers in the field of computer-enhanced analytical chemistry, these advances and emerging research fields would not be possible.

Multi-dimensional separation schemes based on liquid chromatography (LC) coupled to mass spectrometry have gained wide acceptance as effective strategies for the analysis of complex biological mixtures [4]. There are relatively few examples in the literature where the chemical information derived from the separation step is actually used for analyte identification [5], thus for most applications the practical utility of LC–MS is the ability to fractionate the sample, thereby reducing sample complexity and minimizing the effects of chemical noise [6–8]. On the other hand, sample throughput for LC–MS is limited by the LC duty cycle. For example, time-of-flight (TOF) mass analyzers can acquire data at rates of 10–50 kHz (10,000–50,000 spectra s^{-1}), whereas LC separation times range from minutes to hours. While this large time disparity between LC and MS has advantages for signal-averaging of both 1D MS and 2D MS (MS/MS) data, this scheme does not fully utilize the high-rate of data acquisition capabilities of the TOF mass spectrometer.

Ion mobility (IM), a gas-phase electrophoretic separation technique [9–11], can achieve very high separation rates (10^3 Hz) and near 100% duty cycles [12]. Although the peak capacity of IM alone is quite low, the peak capacity of IM-MS is quite high due to the dispersion of analyte ions across two dimensions of analysis, mobility and mass space [13,14]. For example, the peak capacity for IM-MS is the product of the peak capacity of each individual data domain, and the peak capacity of the MS domain is determined by the m/z

* Corresponding author. Tel.: +1 979 845 3345.
E-mail address: Russell@mail.chem.tamu.edu (D.H. Russell).

1387-3806/$ – see front matter © 2008 Elsevier B.V. All rights reserved.
doi:10.1016/j.ijms.2008.11.011

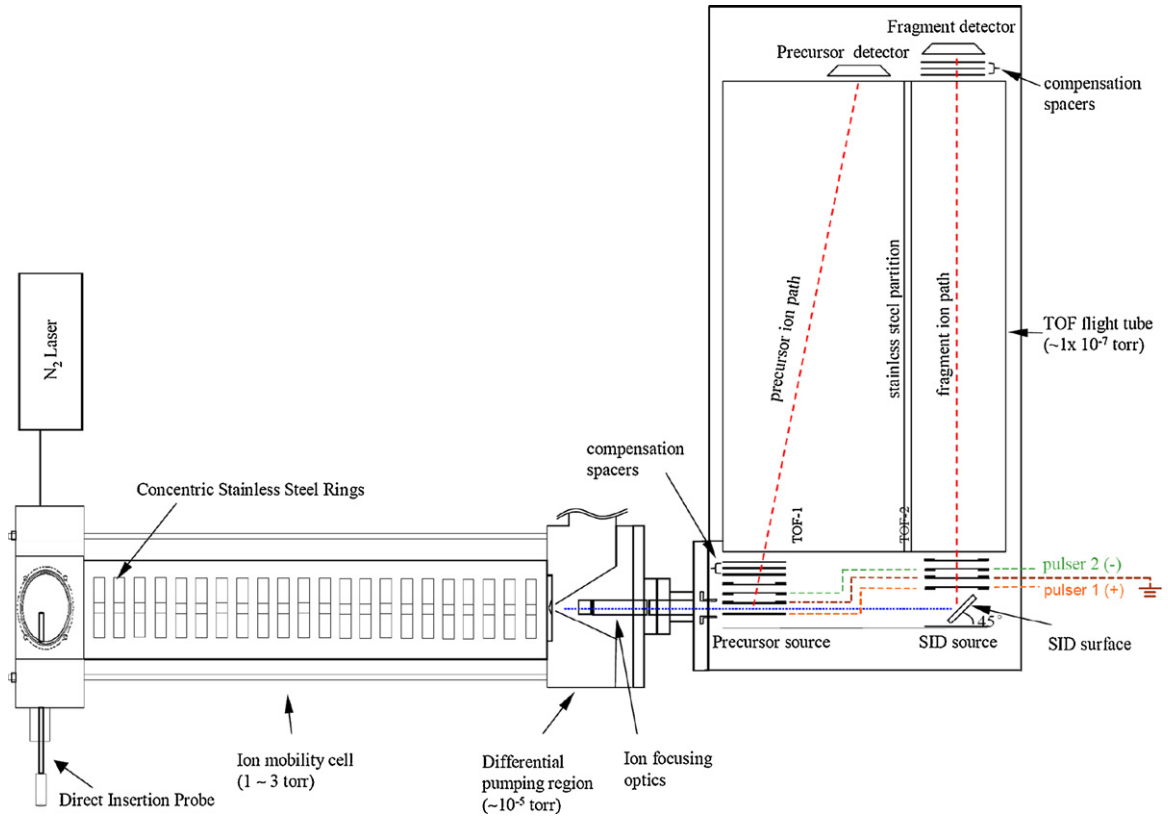

Fig. 1. Schematic diagram of the MALDI-IM-SID-TOF instrument equipped with parallel time-of-flight mass analyzers.

resolution, which is 10^4 or greater for modern TOF instruments. In addition, the peak capacity of IM-MS can be extended further by increasing the dimensionality of the experiment, *i.e.*, IM-MS–MS or chromatography separation prior to IM separation, *i.e.*, LC–IM-MS [15].

IM can be used exclusively as a post-ionization separation technique; however, accurate measurements of the ion arrival-time distributions (ATD) can be used to extract information regarding analyte ion size (effective surface area), which adds another dimension to the experiment. Combining IM with structural mass spectrometry using fragmentation methods such as collision-induced dissociation (CID) [16] and surface-induced dissociation (SID) [17,18] provides a powerful and versatile tool for a wide sample of analytical applications. SID is an especially attractive activation method for proteomics experiments because surface collisions are highly effective at generating sequence informative fragment ions over the m/z range of peptides that result from protein digests (typically 500–3000 m/z) [19], and SID has been shown to be particularly advantageous for the activation of ions formed by laser desorption [20]. Additionally, SID is readily adaptable to orthogonal TOF instrumentation, since orthogonal ion extraction provides a convenient and effective means of recollecting ions that result from collisions with the surface and thus have lost their initial surface directed spatial coherence as a result of the activation event.

We have evaluated several IM-SID-TOF instrument designs in our own laboratory [17,21,22]. In our previous work, we demonstrated the potential for IM-MS using SID to simultaneously generate precursor and fragment ion spectra [17]. With conventional MS based tandem instrumentation (*e.g.*, TOF–TOF, Q-TOF), simultaneous MS and MS/MS data acquisition is not possible owing to the requirement that the first MS stage be scanned across m/z values of interest. The limitation imposed by our previous strategies was the requirement that some fraction of the precursor ions must survive the activation process which hinders the absolute detection limits, *i.e.*, we cannot have 100% conversion of precursor ions to fragment ions. Precursor ion survival in SID is particularly challenging when dealing with a wide range of m/z ions, such as those encountered in protein digest samples, owing to the observation that surface collisional activation deposits a narrow distribution of internal energy into the impacting ions, resulting in a narrow m/z range (~300 m/z) for which sufficient sequence information fragment ion signals are observed [17]. In our previous work we have opted to acquire two sets of data at two different collision energies: one high (40–70 eV laboratory frame) and one low (<10 eV), which negates the inherent advantages of the time-of-flight analysis with regards to sample throughput. Similar issues arise when combining IM-MS with CID. For example, Smith and coworkers incorporated a mobility dependent voltage gradient to the collision region, effectively supplying more energy to larger m/z ions as determined by the observed ion retention times in the IM experiment. Using this technique, a peptide mixture was successfully analyzed with the ability to detect a complete series of fragment ions across the mixture [23]. Clemmer developed a clever online field modulation strategy for an IM-CID-TOF instrument to acquire both precursor and fragment ion spectra by introducing a controllable, high voltage pulse across the CID region [24]. Although such methods allow for tailoring the extent of fragmentation for ions of different m/z, it is difficult to apply similar strategies to the SID-TOF configuration used here since all incident ions experience collisions with the surface prior to ion extraction by the TOF, that is to say, there is no control over which ions are submitted for SID analysis in this type of experimental configuration where the SID surface lies in line with the incident ion beam. Even if a field modulation type experiment is used to manage the extent of ion fragmentation, it would be challenging to correlate the mass analysis of the various mass and energy

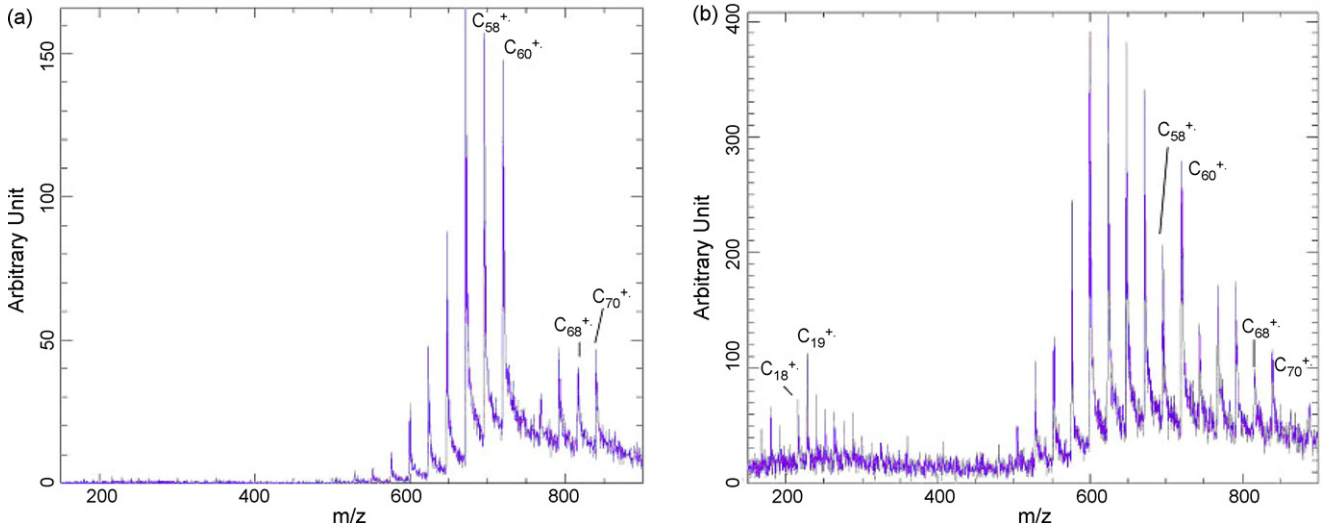

Fig. 2. SID mass spectra of $C_{60}^{\bullet+}$–$C_{70}^{\bullet+}$ acquired with laboratory frame collision energies of (a) 250 eV and (b) 500 eV.

dependent ion scatter trajectories that result from recoil from the surface.

Here, we describe a novel SID instrument configuration aimed at overcoming previous limitations in the multi-dimensional IM-MS experiment while maximizing ion transmission (sensitivity) and data acquisition throughput. The new instrument configuration consists of two separate TOF-1 and TOF-2 mass analyzers, TOF-1 samples intact ions which have been separated in mobility space by the IM drift cell and TOF-2 samples ions that have both eluted from the IM region and recoiled from the SID surface, which allows for the simultaneous mass analysis of mobility separated ions before and after the SID event.

2. Experimental

Fig. 1 contains a schematic of the MALDI-IM-SID-TOF instrument used in this work. The basic instrument was described in our previous paper [22], which has been modified to include two independent TOF mass analyzers. Briefly, ions are formed at the start of a continuously focusing drift cell (30 cm periodic field ion guide) [25,26] via a pulsed nitrogen laser operated at 20 Hz where they

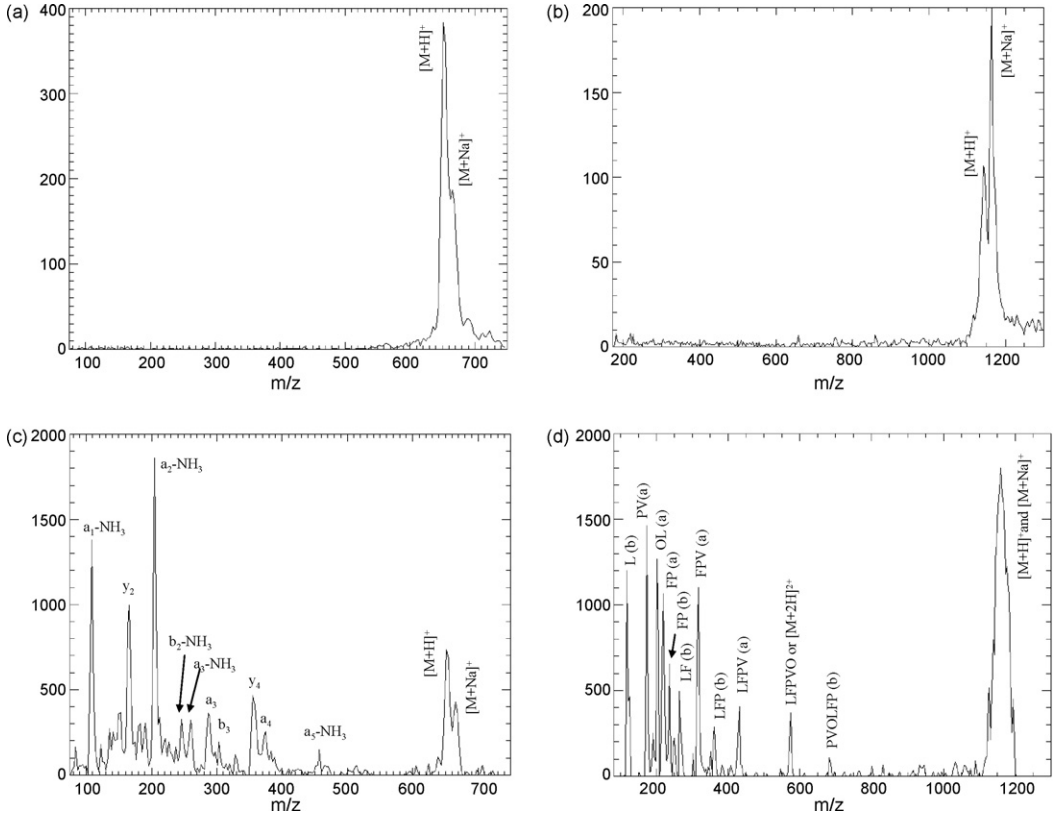

Fig. 3. Precursor (a) and SID (b) mass spectra of RVGVAPG (654.9 m/z) at collisional energy 60 eV, and precursor (c) and SID (d) mass spectra of gramicidin S (cyclic-OLFPVOLFPV, 1141.5 m/z) at collisional energy 90 eV.

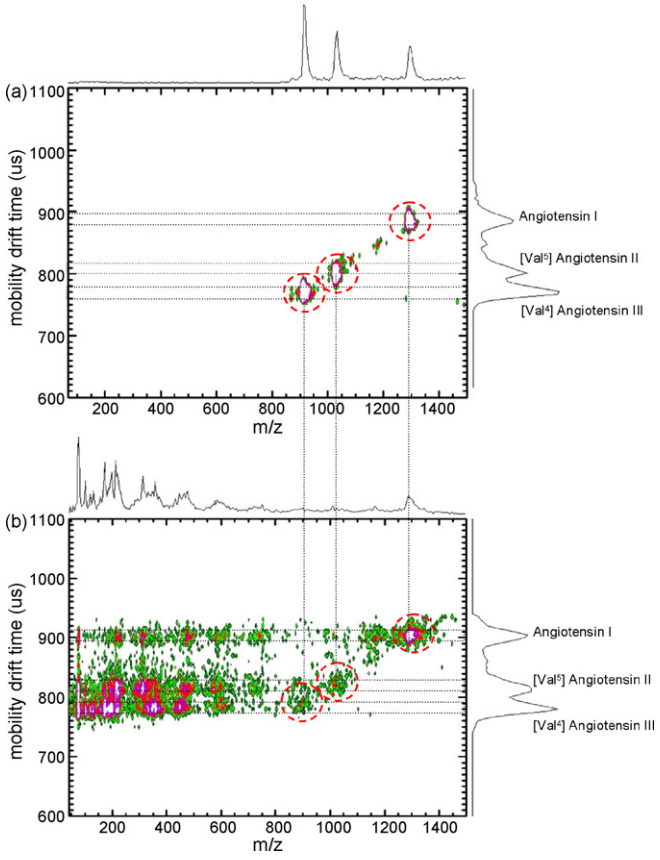

Fig. 4. 2D mobility-mass contour plots of a mixture of angiotensin I (1295.5 *m*/*z*), [Val^5] angiotensin II (1031.2 *m*/*z*), and [Val^4] angiotensin III (916.1 *m*/*z*) obtained (a) on the precursor ion mass analyzer (TOF-1) and (b) on the SID mass analyzer (TOF-2) using a collision energy of 95 eV laboratory frame. The horizontal dotted boxes define the drift time window during which the peptide precursor/fragment mass spectra were acquired. The vertical dotted lines correlate with the precursor ions (circled by red dotted lines) from each spectrum.

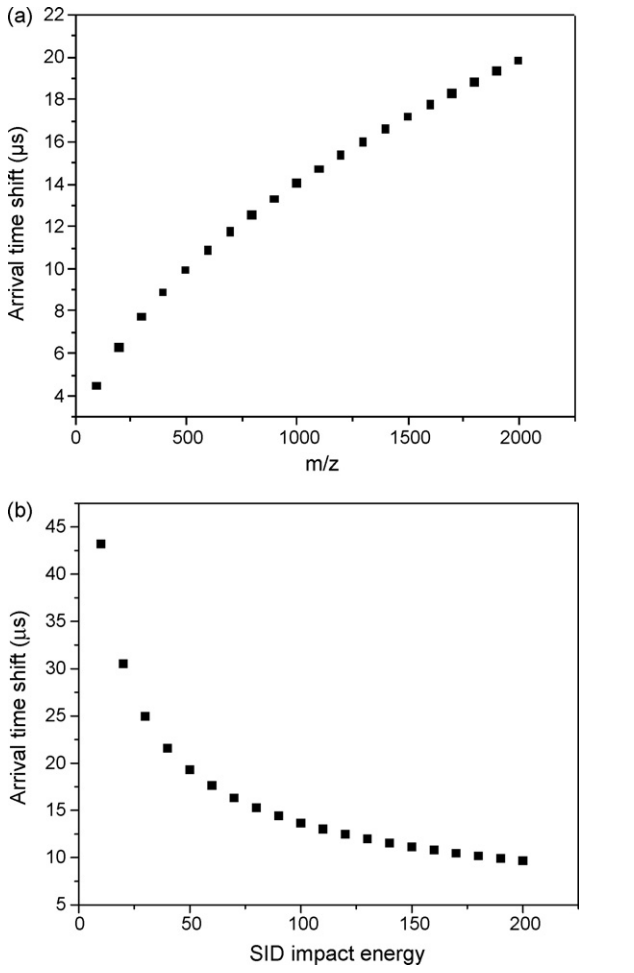

Fig. 5. Calculated arrival time shift as a result of the location difference of the two detectors. (a) Plot for drift time difference *vs.* *m*/*z* at SID impact energy of 95 eV; (b) plot for drift time difference *vs.* SID impact energy for ions of *m*/*z* 1000.

are pulled through the gas filled (~1 Torr He, 25 °C) IM drift cell by means of an applied electric field (~60 V/cm average) where they separate based on their different mobilities. Ions then elute from the drift cell into vacuum, where they are confined and collimated through electrostatic ion optics then transferred and focused between the two parallel ion optical elements of the TOF-1 region. During operation, some ions are extracted by TOF-1, while the remainder pass through and are directed onto an SID surface that lies directly below the TOF-2 ion extraction optics. The orthogonal extraction ion optics and internal TOF chamber was fabricated in-house from austenitic stainless steel (alloy 304). Ion extraction optics for the TOF-1 (labeled 'precursor' ion source in Fig. 1) and TOF-2 (labeled 'SID source' in Fig. 1) are separated by ~6 cm. TOF-1 and TOF-2 analyzers are ~20 cm in length and are equipped with cartridge type microchannel plate (MCP) detectors (25 mm diameter V-stack configuration, Burle Electro-Optics, Inc., Sturbridge). The ion extraction optics for the SID source are off-set to accommodate the SID surface, which is placed in-line with the ion beam, as illustrated in Fig. 1. The collision surface is also canted at a 45° angle relative to the incident ion path, allowing the central (average) trajectory of ion scatter to be directed toward the extraction optics through a high transmission (~90%) electroformed mesh (~120 wire/inch nickel grid, Precision Eforming LLC, Cortland, NY).

Precursor (TOF-1) and SID fragment ion (TOF-2) spectra were acquired by synchronously pulsing the ion extraction voltages at a rate of 20 kHz. Optimization of the pulse frequency is discussed below. An extraction potential of 600 V (absolute magnitude) was used for both TOF extraction pulses, and the bias on both TOF chambers was set at −5 kV relative to ground potential. Signals from each TOF detector are acquired using a multi-channel (eight independent channels) time-to-digital converter (TDC, Ionwerks, Houston, TX). The TOF data sets are reassembled to yield 3D data (IM arrival-time distributions, precursor and SID fragment ion abundances) plots using custom data processing software (Ionwerks, Houston, TX) produced with the IDL development language (ITT Visual Information Solutions, Boulder, CO). The SID impact energy can be varied, as defined by the potential difference between the exit of the drift cell (where ions exit at near thermal energies) and the SID surface.

The peptide RVGVAPG (MW 654.8 Da) was synthesized in-house using conventional Fmoc chemistry on solid support. Gramicidin S (cyclic-OLFPVOLFPV, 1141.5 Da) was purchased from Enanta Pharmaceuticals Inc. (Watertown, MA). Angiotenisin I (DRVYIHPFHL, 1295.7 Da), [Val^5]-angiotensin II (DRVYVHPF, 1045.5 Da), [Val^4]-angiotensin III (RVYVHPF, 916.1 Da) and horse heart cytochrome c were purchased from Sigma (St. Louis, MO). Sequence grade trypsin (Promega, Madison, WI) was used in a 40:1 (w/w) analyte-to-trypsin ratio. All of the peptides and proteins were used without further purification. The α-cyano-4-hydroxycinnamic acid (CHCA) used as a MALDI matrix was purchased from Sigma and recrystallized several times prior to use. MALDI samples were prepared using the standard dried droplet technique using a 50% methanol/water solution in a matrix-to-analyte ratio of 1000:1. For the studies of model peptides approximately 25 pmol of sample was deposited onto the MALDI sample stage, and for the analysis of protein

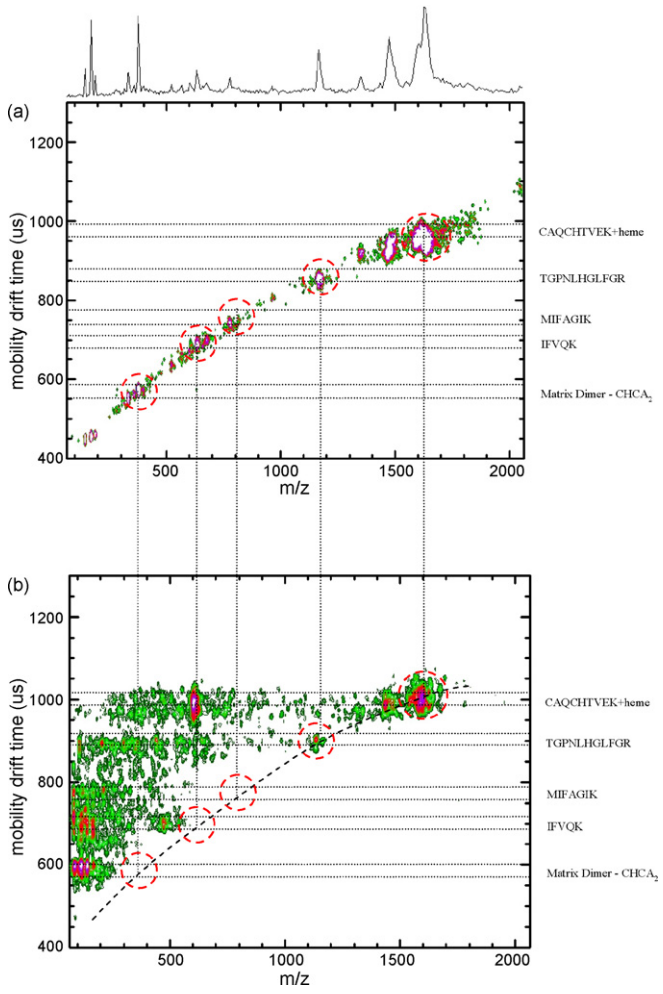

Fig. 6. 2D mobility–mass contour plots of an "in solution" tryptic digest of cytochrome *c* obtained (a) on the precursor ion mass analyzer (TOF-1) and (b) on the SID mass analyzer (TOF-2) using a collision energy of 95 eV laboratory frame. Ion signals are labeled to the right of their corresponding drift times. The horizontal dotted boxes define the drift time window during which the peptide precursor/fragment mass spectra were acquired. The vertical dotted lines correlate the precursor ions (circled by red dotted lines) from each spectrum.

digests the equivalent of approximately 10 pmol of protein was deposited.

3. Results and discussion

Here, we describe a prototype dual-source/dual-detector-IM-SID-TOF instrument specifically designed to establish proof-of-concept for post-ionization separation and simultaneous acquisition of precursor and SID fragment ion spectra for high-throughput analysis of peptides. An obvious limitation of the prototype instrument is the use of linear, low resolution TOF analyzers. Similar experiments can be performed using reflectron-based TOF instruments; however, the design criteria (*i.e.*, spatial array detection) necessary for achieving high resolution and accurate mass measurement using a reflectron TOF are not yet completed.

Several factors must be taken into account when operating a dual TOF for simultaneous acquisition of precursor and fragment ion data. For example, the ion source and detector for TOF-1 must be properly positioned to insure that ions having a large range of kinetic energies strike the detector. That is, ions extracted into TOF-1 have velocity vectors composed of both axial (beam axis) and transverse (orthogonal, TOF axis) components, thus the detector must be precisely placed to collect the ions. For example, the laboratory collision energies required to fragment fullerene ions ($C_{60}^{\bullet+}$ and $C_{70}^{\bullet+}$) range from ~200 to ~1000 eV (Fig. 2), whereas peptide ions and small organic molecular ions (<2000 amu) require kinetic energies of less than 100 eV. Because the optimum SID impact energies for a specific precursor ion m/z is quite narrow, it is useful to utilize several impact energies across the range of masses desired, and to achieve this TOF-1 must be able to mass analyze ions over a range of kinetic energies without compromising instrument sensitivity and/or mass resolution. Ion trajectories for a range of ion kinetics were computed using SIMION and we found that a 25 mm MCP detector offset axially by 40 mm from the extraction optics (measured from center-to-center) collected a large fraction (>90%) of the ions, and experimentally we found that this configuration also collected a wide range of ion kinetic energies (25–450 eV laboratory frame); however, it should be noted that a decrease in sensitivity is observed for both extremes of the kinetic energy range. It should also be noted that for the peptide samples analyzed in this work, the incident energy used is normally between 40 and 120 eV for extensive fragmentation, thus there is no need to change the axial distance between the TOF-1 ion source and detector to accommodate the kinetic energy requirements for different analytes. The placement of the TOF-2 detector is much less complicated because ions that enter the extraction region and are scattered from the surface have relatively low axial velocities. In fact, we found that a detector placed directly above the extraction source collects >90% of the fragment ions extracted from the TOF-2 ion source.

The sensitivity limit for this instrument is determined by the number of ions that enter and are detected by TOF-2, and these limits are determined by the duty-cycle for ion extraction by TOF-1, *i.e.*, the fraction of the ions that are required to obtain a reasonable S/N ratio for the precursor ion signal, the fraction of ions entering TOF-2 and the efficiency for SID, *i.e.*, efficiency for conversion of precursor-to-fragment ions. Thus, careful consideration must be given to the relative acquisition rates of the two TOF analyzers to ensure that TOF-1 is not oversampling the ion beam. The efficiency of precursor-to-fragment ion conversion is estimated to range from 5–20% [27], thus a greater fraction of ions must be sampled by TOF-2 than for TOF-1. We first estimated the optimum TOF-1 acquisition rate by assuming that TOF-1 is sampling ions from a continuous beam and that no ions are lost during the rise and fall of the TOF extraction pulse. The ion extraction regions of TOF-1 and TOF-2 are separated (center-to-center) by ~60 mm, thus an ion of m/z 2000 and a kinetic energy of 80 eV would traverse this distance in approximately 20 μs. If TOF-1 is operating at 20 kHz, *e.g.*, 50 μs between extraction pulses, then ions are extracted from the beam 40% of the time (20 μs/50 μs). Under these conditions approximately 60% of the ions are transferred to TOF-2. The numbers of ions sampled by TOF-2 can be increased simply by decreasing the sampling rate of TOF-1.

The utility of the dual TOF system for peptide mass mapping and amino acid sequence determination was evaluated using a series of model peptides. Fig. 3a and b contain data for the peptide RVGVAPG. Note that intact ions ($[M+H]^+$ and $[M+Na]^+$) are observed in the precursor ion spectrum (Fig. 3a), whereas the dominant ion signal in the SID spectrum corresponds to fragment ions resulting from the 70 eV impact of ions upon the surface (Fig. 3b). The fragmentation efficiency of this peptide at 70 eV is approximately 80%, as determined by the ratio of total fragment ion signal (obtained by TOF-2) to precursor ion signal (TOF-1). Similar results were obtained for gramicidin S. Note, however, that for gramicidin S both precursor and fragment ions are detected in the SID-TOF spectrum (Fig. 3d) at impact energies of 90 eV. We also detected a high abundance of precursor ions for gramicidin S in our previous SID studies and attributed this observation to the relatively higher energy necessary to fragment cyclic peptide ions [18].

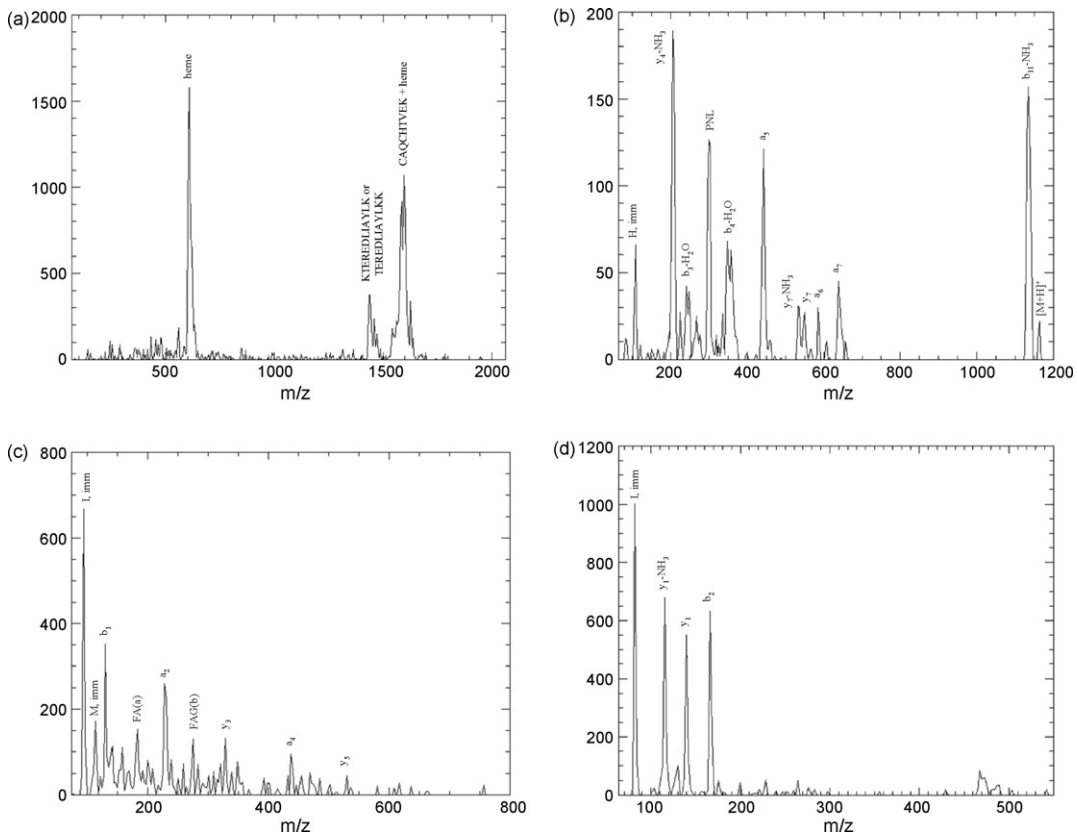

Fig. 7. SID mass spectra of the four most abundant peptides from an "in solution" tryptic digest of cytochrome *c* acquired at a laboratory frame collisional energy of 95 eV: (a) CAQCHTVEK + heme at the drift time of 1000 ± 20 μs, *m*/*z* of $[M+H]^+$ 1634; (b) TGPNLHGLFGR at the drift time of 900 ± 20 μs, *m*/*z* of $[M+H]^+$ 1169; (c) MIFAGIK at the drift time of 780 ± 20 μs, *m*/*z* of $[M+H]^+$ 779; (d) IFVQK at the drift time of 700 ± 20 μs, *m*/*z* of $[M+H]^+$ 634.

It is also interesting to note that precursor ion signals observed in TOF-1 mass spectrum is of much higher resolution than are precursor ion signals detected in the TOF-2 spectrum. One explanation for the higher resolution for TOF-1 is differences in the initial position of ions that are sampled by TOF-1, *i.e.*, these ions are extracted orthogonally from a relatively narrow (collimated) ion beam, whereas ion extracted by the SID source are extracted from population of ions that are scattered from the SID surface which comprise a larger kinetic energy distribution. This lower mass resolution in the SID spectrum may also be a consequence of sampling precursor ions undergoing unimolecular dissociation following surface activation on a timescale (~1 μs) comparable to the ion's residence time in the ion source [28].

The utility of the dual TOF IM-MS instrument for high-throughput applications is illustrated by analyzing a three component peptide mixture composed of angiotensin I, $[Val^5]$-angiotensin II and $[Val^4]$-angiotensin III. Fig. 4 contains 2D plots of the resulting data from both TOF regions, projecting the mobility drift time on the *y*-axis and the *m*/*z* ratio on the *x*-axis. Fig. 4a contains the data taken using TOF-1. Note that the peptide ion signals are clearly separated in both the mobility and mass dimensions and are virtually free of chemical noise. Fig. 4b contains the spectrum obtained using TOF-2. Because IM separation occurs prior to SID the mobility drift times of the fragment ions are the same as that for the precursor ion, *i.e.*, the SID fragment ions can be correlated to a specific precursor ion. The 2D projection contained in Fig. 4b illustrates another key feature of this manner of analysis (*e.g.*, pre- and post-ion activation mass analysis following ion mobility separation). The mass spectrum contained in Fig. 4b is highly congested. On the other hand, the 2D projection clearly partitions the fingerprint fragment ions of each peptide.

Using surface impact energies that yield sufficient ion signal for each precursor ion, the 2D mobility-mass correlation plot yields an adequate amount of information to identify both the parent ion mass (mass mapping) and sequence (mass fingerprinting); however, because SID efficiency is mass dependent, a single SID impact energy will not be optimum for the full range of peptide *m*/*z* values sampled in a typical tryptic digestion. This is illustrated by the data contained in Fig. 4b where SID was performed using 95 eV surface impact energy. Although ion signals observed for the highest *m*/*z* ion in the mixture, angiotensin I, contains abundant precursor and fragment ion signals, the precursor ion signals for the small peptide ions, $[Val^5]$-angiotensin II and $[Val^4]$-angiotensin II, are depleted by SID, thus compromising the peptide mass mapping data.

In principle it should be possible to acquire precursor ion spectra using TOF-1 and all SID fragment ion spectra using TOF-2; however, the mobility drift times for TOF-2 ions would be shifted owing to the time required to traverse the distance between (60 mm) the two ion sources. The difference in drift time in this region is both mass and kinetic energy dependant and can be estimated by generating correlation curves for different *m*/*z* values (Fig. 5a) and collision energies (Fig. 5b). For the collision energy used here (95 eV), the calculated drift time shifts for the three peptide masses are approximately ~16.1 μs, ~14.2 μs, and ~13.4 μs for $[Val^4]$-angiotensin III, $[Val]^5$-angiotensin II, and angiotensin I, respectively, which correlate well to the experimental drift time shifts observed. By applying the appropriate time corrections, the empirical data can be directly correlated. It should be noted, however, that extrapolation of the apparent drift time to intersect the peptide trendline is potentially subject to significant errors owing to deviations in peptide ion conformation space [29].

Table 1
A list of tryptic peptides from cytochrome *c* (horse) detected by the precursor detector.

Sequence	Observed m/z	Calculated m/z ($[M+H]^+$)	Start–end
GITWK	604.3	604.3	56–60
IFVQK	635.1	634.4	9–13
MIFAGIK	779.2	779.4	80–86
EDLIAYLK	964.5	964.5	92–99
TGPNLHGLFGR	1168.4	1168.6	28–38
TEREDLIAYLK	1349.9	1350.7	89–99
TEREDLIAYLKK	1478.2	1478.8	89–100
or KTEREDLIAYLK	1478.2	1478.8	88–99
KTGQAPGFTYTDANK	1598.1	1598.8	39–53
CAQCHTVEK + heme	1634.3	1634.1	14–22 + heme

The utility of the dual TOF-SID apparatus for proteomics studies is illustrated by data contained in Fig. 6. Fig. 6a contains the 2D IM-MS data obtained from a tryptic digest of cytochrome *c*; Fig. 6a contains only TOF-1 ion signals from nine peptides (see Table 1) and a matrix dimer. TOF-2 ion signals for the four most abundant peptide ions along with the matrix dimer are correlated in Fig. 6b. The peptide ion signal observed at the longest mobility drift time (~1000 μs) corresponds to m/z of 1634.3, which could be CAQCHTVEK-heme or IFVQKCAQCHTVEK ($[M+H]^+$ 1635.0). However, the abundant SID fragment ion signal at m/z 616.0 indicative of heme supports the assignment as CAQCHTVEK-heme (Fig. 7a). We previously showed that the tryptic heme containing peptide ion of CAQCHTVEK-heme fragments to lose the heme group [21]. The peak corresponding to the second longest mobility drift time is assigned to the $[M+H]^+$ ion of the tryptic peptide TGPNLHGLFGR (m/z 1168.4), and 10 corresponding fragment ions derived from *a*-, *b*-, and *y*-type ions are observed in the SID spectrum (Fig. 7b). The remaining ion signals corresponding to shorter drift times were also assigned in the same manner; these ions are assigned to the tryptic peptides MIFAGIK ($[M+H]^+$ 780.0, Fig. 7c) and IFVQK ($[M+H]^+$ 634.4, Fig. 7d). Because these two low mass peptides were completely fragmented using a collision energy of 95 eV, no precursor ion signals are observed in the SID spectrum alone, making it difficult to sequence this peptide without the complimentary precursor ion spectrum from TOF-2. Finally, the matrix dimer ($CHCA_2$) at m/z 379 might be confused as a peptide ion in the SID spectrum if the precursor data was not also provided, further illustrating the utility of acquiring both sets of data, precursor and fragment ion spectra, in the same experiment.

4. Conclusions

The use of a parallel TOF arrangement in a MALDI-IM-SID-TOF instrument enables simultaneous acquisition of MS and tandem MS spectra. Peptide sequencing experiments based upon this dual TOF design are enhanced with the precursor mass data, information that is normally compromised at efficient SID energies where high sequence coverage comes at a loss of precursor mass signal. The higher mass resolution of the precursor TOF as compared with the SID-TOF facilitates accurate mass assignments of the precursor mass. The observed lower mass resolution for the SID-TOF can be explained as a result of sampling a wide spatial and energetic distribution of ions from the surface, or of late fragmenting "survivor" ions from the SID surface, or a combination of both effects. The precursor TOF geometry is capable of orthogonally extracting ions across a large range of surface impact energies (25–450 eV) without the need to adjust any instrument settings, facilitating the simultaneous acquisition of precursor and fragment ion data in the same experimental run. The difference in mobility drift time observed between the precursor and SID mass analyzers resulting from differences in ion arrival times is both energy and mass dependent, and can be predicted and corrected for using arrival time correlation curves.

Acknowledgements

Funding support for this work was provided by the U.S. Department of Energy Division of Chemical Sciences, BES (DE-FG02-04ER15520), the National Science Foundation (CHE-0521216), the National Institutes of Health (1R01 RR01958701), and the Robert A. Welch Foundation (A-1176). The authors would also like to acknowledge Tom Egan of Ionwerks, Inc. (Houston, TX) for his assistance with the details regarding the synchronization of the two TOF data acquisition scheme.

References

[1] C.L. Wilkins (Ed.), Computer-Enhanced Analytical Spectroscopy, vol. 4, Plenum Press, New York, 1993, p. 308.
[2] C.L. Wilkins, J.O. Lay Jr. (Eds.), Identification of Microorganisms by Mass Spectrometry, John Wiley & Sons, Inc., New York, 2006, p. 352.
[3] J.O. Lay Jr., R. Liyanage, S. Borgmann, C.L. Wilkins, Trends Anal. Chem. 25 (2006) 1046.
[4] Y. Ishihama, J. Chromatogr. A 1067 (2005) 73.
[5] R.D. Smith, Y. Shen, K. Tang, Acc. Chem. Res. 37 (2004) 269.
[6] S.P. Gygi, B. Rist, S.A. Gerber, F. Turecek, M.H. Gelb, R. Aebersold, Nat. Biotechnol. 17 (1999) 994.
[7] E.K. Fridriksson, A. Beavil, D. Holowka, H.J. Gould, B. Baird, F.W. McLafferty, Biochemistry 39 (2000) 3369.
[8] O. Kaiser, D. Bartels, T. Bekel, A. Goesmann, S. Kespohl, A. Pühler, F. Meyer, J. Biotechnol. 106 (2–3) (2003) 121.
[9] R.H. St. Louis, H.H. Hill, Crit. Rev. Anal. Chem. 21 (1990) 321.
[10] G.A. Eiceman, Crit. Rev. Anal. Chem. 22 (1991) 471.
[11] J.A. McLean, B.T. Ruotolo, K.J. Gillig, D.H. Russell, Int. J. Mass Spectrom. 240 (2005) 301.
[12] J.A. McLean, W.K. Russell, D.H. Russell, Anal. Chem. 75 (3) (2003) 648.
[13] B.T. Ruotolo, K.J. Gillig, E.G. Stone, D.H. Russell, J. Chromatogr. B 782 (2002) 385.
[14] J.A. McLean, D.H. Russell, Int. J. Ion Mob. Spec. 8 (1) (2005) 66.
[15] S. Henderson, S.J. Valentine, A.E. Counterman, D.E. Clemmer, Anal. Chem. 71 (1999) 291.
[16] C.S. Hoaglund-Hyzer, D.E. Clemmer, Anal. Chem. 73 (2001) 177.
[17] V.H. Wysocki, K.E. Joyce, C.M. Jones, R.L. Beardley, J. Am. Soc. Mass Spectrom. 199 (2008) 190.
[18] E.G. Stone, K.J. Gillig, B.T. Ruotolo, D.H. Russell, Int. J. Mass Spectrom. 212 (2001) 519.
[19] R.D. Smith, Comp. Funct. Genom. 3 (2002) 143.
[20] C.F. Ijames, C.L. Wilkins, Anal. Chem. 62 (1990) 1295.
[21] E.G. Stone, K.J. Gillig, B.T. Ruotolo, K. Fuhrer, M. Gonin, A. Schultz, D.H. Russell, Anal. Chem. 73 (2001) 2233.
[22] W. Sun, J.C. May, D.H. Russell, Int. J. Mass Spectrom. 259 (2007) 79.
[23] E.S. Baker, K. Tang, W.F. Danielson III, D.C. Prior, R.D. Smith, J. Am. Soc. Mass Spectrom. 19 (3) (2008) 411.
[24] S.L. Koeniger, S.J. Valentine, S. Myung, M. Plasencia, Y.J. Lee, D.E. Clemmer, J. Proteome Res. 4 (2005) 25.
[25] K.J. Gillig, B.T. Ruotolo, E.G. Stone, D.H. Russell, Int. J. Mass Spectrom. 239 (1) (2004) 43.
[26] K.J. Gillig, D.H. Russell, U.S. Patent 6,639,213 (2003).
[27] B. Winger, H.-J. Laue, S. Horning, R. Julian, S. Lammert, D. Riederer Jr., R.G. Cooks, Rev. Sci. Inst. 63 (12) (1992) 5613.
[28] C.M. Gamage, F.M. Fernandez, K. Kuppannan, V.H. Wysocki, Anal. Chem. 76 (17) (2004) 5080.
[29] L. Tao, J.R. McLean, D.H. Russell, J. Am. Soc. Mass Spectrom. 18 (7) (2007) 1221.